ARTICLE

OBC
www.rsc.org/obc

Flexible self-assembling porphyrin supramolecules

Ken D. Johnstone,[a] Kentaro Yamaguchi[b] and Maxwell J. Gunter*[a]

[a] *School of Biological, Biomedical and Molecular Sciences, University of New England, Armidale, N.S.W. 2350, Australia. E-mail: mgunter@une.edu.au; Fax: 612-6773-2368; Tel: 612-6773-2767*

[b] *Faculty of Pharmaceutical Sciences at Kagawa Campus, Tokushima Bunri University, 1314-1 Shido, Sanuki-city, Kagawa 769-2193, Japan. E-mail: yamaguchi@kph.bunri-u.ac.jp; Fax: +81-873-894-0181; Tel: 81-87-894-5111(ext 6313)*

Received 18th May 2005, Accepted 8th June 2005
First published as an Advance Article on the web 4th July 2005

The design and chemical synthesis of a series of hybrid flexible self-assembling supramolecules utilising both crown ether–naphthalene diimide host–guest chemistry and metalloporphyrin–pyridyl coordination is discussed. The resulting compound structures and dynamics are probed using a variety of techniques, including diffusion ordered NMR spectroscopy (DOSY) and cold-spray ionisation mass spectrometry (CSI-MS).

Introduction

The recent interest and potentially huge technological opportunities associated with the miniaturization of components for electronic devices has driven supramolecular chemists to embrace the challenge of designing molecular scale machines. Two promising supramolecular topologies that have been extensively explored as useable molecular scale machines are rotaxanes[1] and catenanes.[2] These multi-component systems are held together mechanically and, in the case of those constructed as molecular switching devices, often utilise subtle secondary interactions in their assembly to drive their switching motion. The study of these systems has led to the invention of a variety of more complex, hybrid topologies, such as daisy chains,[3,4] polyrotaxanes[4,5] and polycatenanes[6] with different and interesting new characteristics.

We have recently investigated a series of rotaxane systems both in solution and on ArgoGel™ beads.[7,8] These systems, comprised of aromatic crown ether *loop* components encircling pyridyl substituted naphthalene diimide *thread* components with bulky metallo–porphyrin *stopper* components, are held together by a series of secondary interactions. A combination of hydrogen bonding, π–π and charge transfer interactions stabilise the crown ether–naphthalene diimide host–guest binding interaction, while coordination between the terminal pyridyl ligands, built into the structure of the naphthalene diimide thread, and the metallated porphyrin stoppers enable the stoppering of the thread to prevent release of the trapped crown ether component. Since all of the interactions are reversible and the rotaxane is the most stable thermodynamic product, the system self-assembles in solution through the simple mixing of the individual components (Fig. 1). Because the entire assembly process is

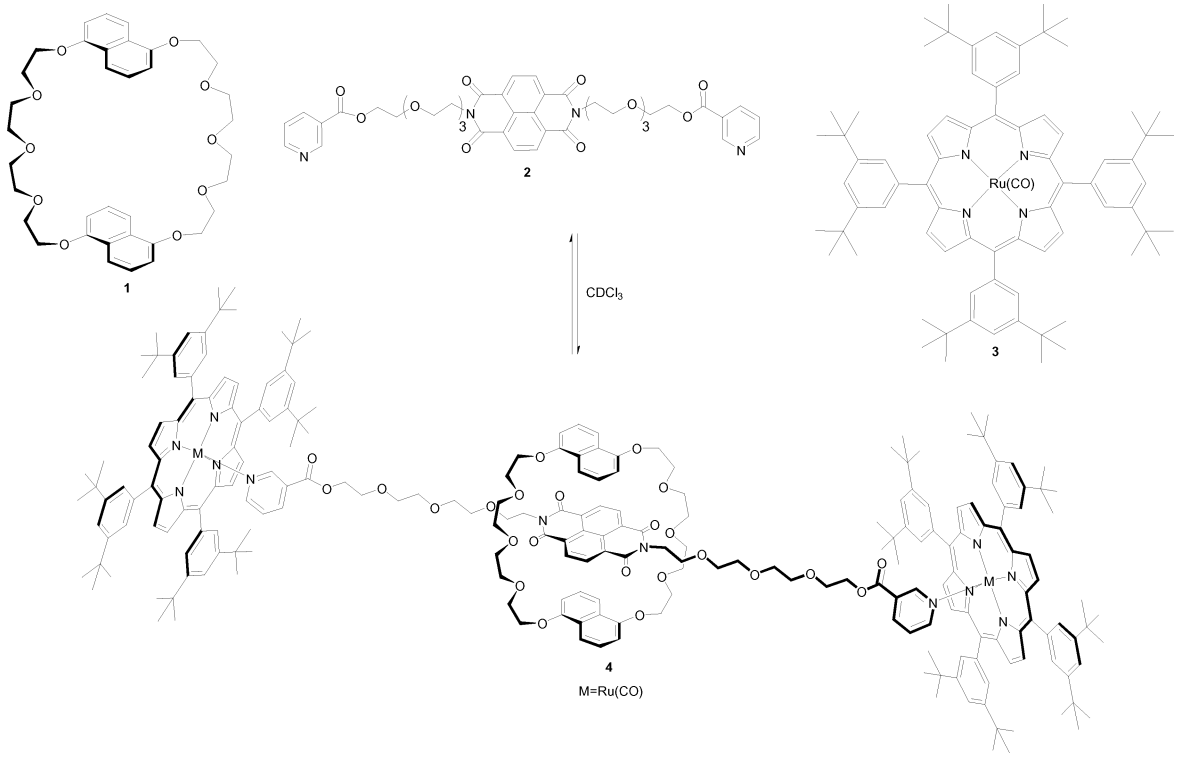

Fig. 1 The dinaphthalene crown ether macrocycle **1**, naphthalene diimide thread **2** and ruthenium carbonyl porphyrin stopper **3** assemble to form the thermodynamically most stable product rotaxane **4** when mixed in solution.

DOI: 10.1039/b506987d

governed by various equilibria, the conditions of the systems can be modified to improve the efficiency and outcome of the system, affording a greater yield of the desired supramolecular assembly. This phenomenon has the potential to enable the rapid and simple construction of quite complex supramolecular architectures that would otherwise be problematic to synthesise using traditional kinetic-controlled supramolecular synthetic techniques.

Our aim was to modify the different components of the rotaxane system to enable their permanent covalent attachment to each other, in order to construct a series of new, increasingly complex supramolecular systems. Attachment of the rotaxane thread component to the loop component to yield the daisy chain or hermaphrodite-type compound **5** was expected to either self-complex or form complex oligomeric structures through intermolecular interactions. Subsequent incorporation of the ruthenium carbonyl porphyrin **3** into the system would act to stopper the products, forming species such as **7** (Scheme 1). Covalent attachment of the rotaxane thread component to a metalloporphyrin stopper to form the hybrid compound **6** was expected also to either self-complex or form oligomeric macrocyclic structures, which upon addition of dinaphthalene crown ether **1** would reversibly form various catenane species, such as **8** (Scheme 2).

Results and discussion

Synthesis

The daisy chain monomer **5** was synthesised by coupling mono-functionalised crown **9** with mono-functionalised thread **11** *via* an ester linkage (Scheme 1). Both mono-functionalised components were chosen for their synthetic simplicity and proven potential for complexation.[9] The mono-functionalised crown **9**, composed of both naphthalene and functionalised benzo aromatics, was synthesised in five steps from commercially available material, utilising methodology developed by Sanders and co-workers.[9] The mono-functionalised thread **11** was made by reacting **10** with one eq. of nicotinic acid and separation of the resulting product mixture. Naphthalene diimide **11** was designed to have terminal pyridyl functionality to allow subsequent coordination experiments with metallated porphyrin stoppers.

The catenane precursor **6** was synthesised by fusing porphyrin **13** and thread **11** components *via* an ester linkage, followed by ruthenium carbonyl insertion with triruthenium dodecacarbonyl in refluxing toluene (Scheme 2). The porphyrin subunit **13** was synthesised in two steps from commercially available material. Firstly a mixed aldehyde condensation with pyrrole in refluxing propionic acid to form **12**, followed by reaction with succinic anhydride, DMAP and NEt_3 in dichloromethane to form **13**. The mono-functional tolyl porphyrin **13** was used as a component of **6** as it proved easier to synthesise on larger scales than mono-functional di-(*t*-butyl)phenyl porphyrin analogues.

NMR structure elucidation

Thread-crown hybrid. The structural conformation of **5** in solution was obtained primarily using proton NMR, C–H correlation spectroscopy, gradient COSY, NOESY and ROESY techniques. Scheme 1 shows the non-systematic numbering system used to compare the precursors, **9** and **11**, and the target compound, **5**.

Interesting chemical shift differences in the ^{1}H NMR spectra were noted between **5** and its precursors, **9** and **11** (Fig. 2). The single diimide peak ($H_{a,b,c,d}$) was shifted upfield from δ 8.76 in **11** to δ 8.65 in **5**. Likewise, the crown aromatic peaks (H_{i-q}) were shifted significantly upfield. H_n and H_q were shifted from δ 7.86 to δ 7.55, H_m and H_p were shifted from δ 7.30 to δ 7.11,

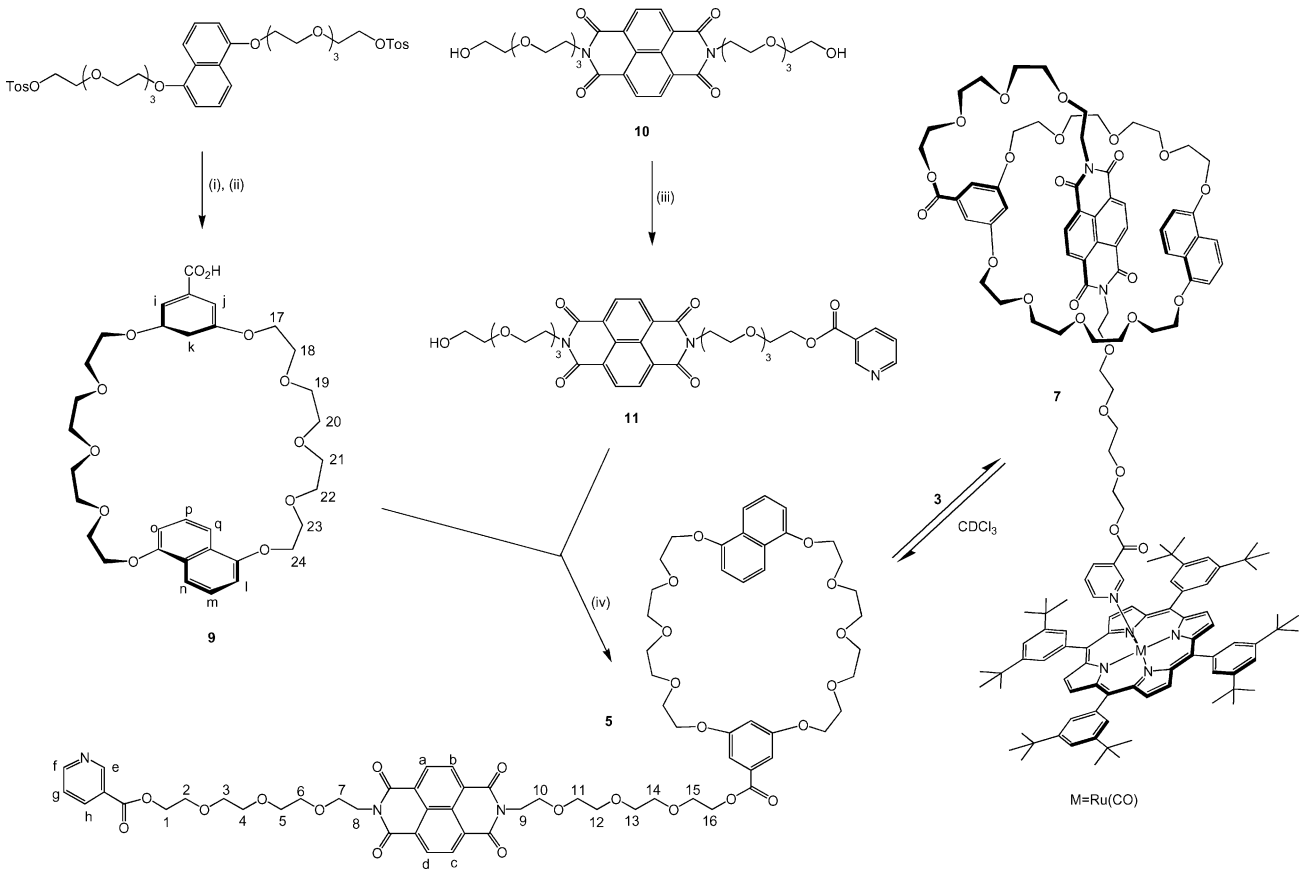

Scheme 1 *Reagents and conditions*: (i) methyl 3,5-dihydroxybenzoate, K_2CO_3, acetone, reflux, 26%; (ii) 2 M NaOH, glycerol, reflux, 57%; (iii) nicotinic acid, HOBT, EDC, NEt_3, DCM, rt, 33%; (iv) HOBT, EDC, NEt_3, DCM, rt, 43%. Also shown is the non-systematic numbering system used for NMR proton assignment of **5** and its precursors, **9** and **11**.

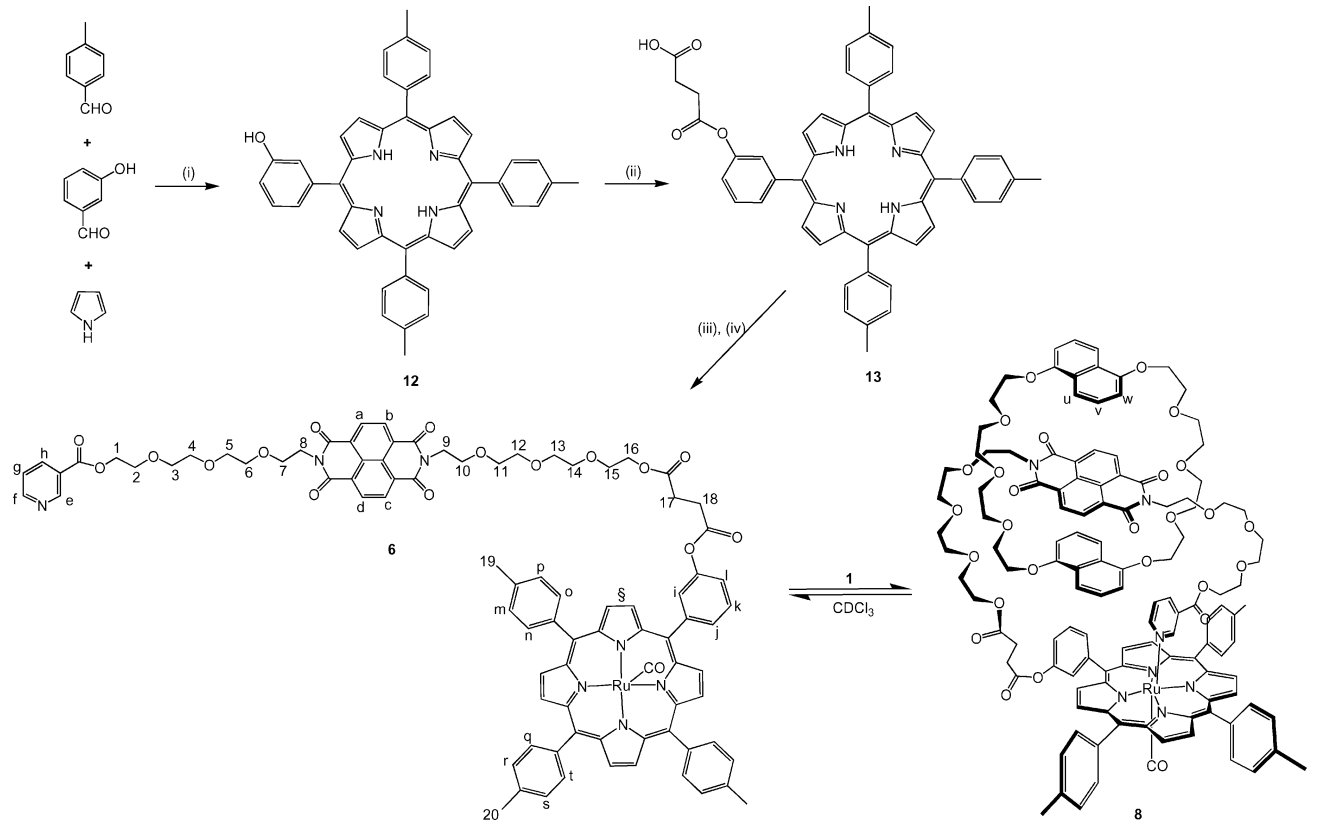

Scheme 2 *Reagents and conditions*: (i) propionic acid, reflux, 3%; (ii) succinic anhydride, DMAP, NEt_3, DCM, 73%; (iii) HOBT, EDC, NEt_3, DCM, 51%; (iv) $Ru_3(CO)_{12}$, toluene, reflux, 52%. Also shown is the non-systematic numbering system used for ^{1}H NMR comparison of **6** and its precursors, **11** and **16**.

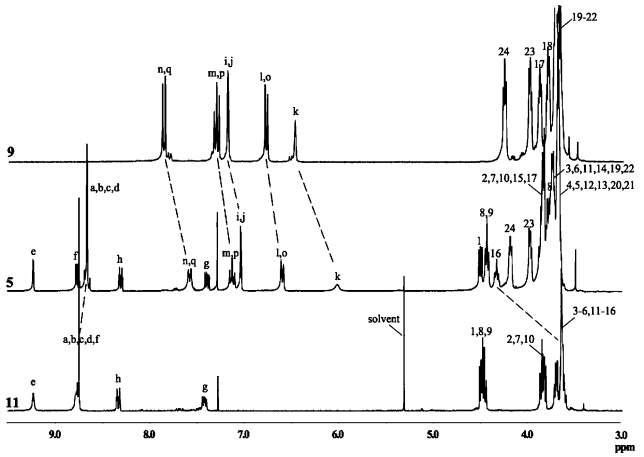

Fig. 2 ^{1}H NMR comparison at 30 °C of precursors **9** (top), **11** (bottom) and target compound **5** (middle) in $CDCl_3$. Significant chemical shift changes are highlighted with dashed lines.

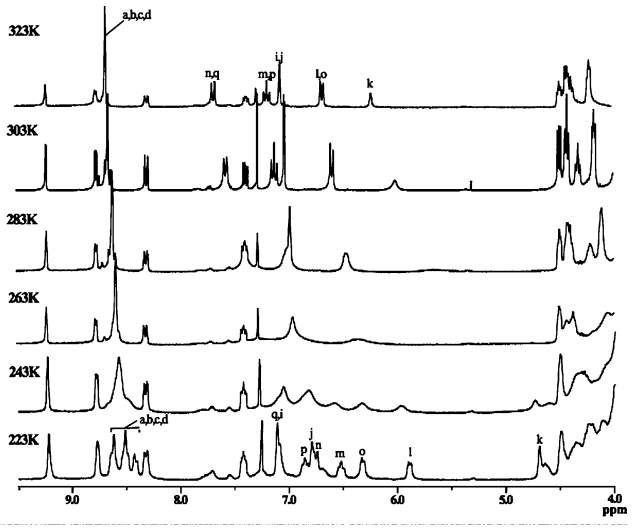

Fig. 3 ^{1}H NMR temperature comparison for **5** in $CDCl_3$. Corresponding sample temperatures are indicated on the left. Proton peaks that significantly shift over the temperature range are highlighted with labels.

H_l and H_o were shifted from δ 6.77 to δ 5.58, H_i and H_j were shifted from δ 7.19 to δ 7.02 and H_k was shifted from δ 6.47 to δ 5.99 in **9** and **5**, respectively. These upfield shifts are indicative of aromatic shielding effects resulting from a crown–diimide interaction. The observed single set of sharp peaks are indicative of a fast-exchanging process, resulting in time-averaged shifts of complexed and uncomplexed crown and diimide at 30 °C; a similar behaviour that we have observed previously for related pseudorotaxane systems.[7] Fig. 2 also highlights a downfield, deshielded shift in the position of H_{16}, the proton closest to the new ester linkage of **5**, which shifts from δ 3.54–3.73 in **11** to δ 4.28 in **5**.

Variable temperature NMR experiments proved particularly useful in studying the dynamic behavior of **5** (Fig. 3). The diimide peak ($H_{a,b,c,d}$) shifts upfield with lower temperature, as the more shielded, complexed species becomes predominant in solution, and splits into three individual peaks at low temperatures (−40 °C (223 K) and below) as the exchange between each diimide proton is slowed sufficiently on the NMR time scale. The diimide peak varies from a singlet (δ 8.67) at 50 °C (323 K) to three broad peaks (δ 8.62, δ 8.52 and δ 8.43) at −50 °C (213 K).

The crown aromatic naphthalene peaks (H_{l-q}) also shift upfield as the aromatic-shielded complex becomes more predominant in solution. At 50 °C (323 K) three crown naphthalene peaks at δ 7.67 ($H_{n,q}$), δ 7.18 ($H_{m,p}$) and δ 6.67 ($H_{l,o}$) change, at −50 °C (223 K), to six individual peaks at δ 7.12 (H_q), δ 6.86 (H_p), δ 6.75 (H_n), δ 6.53 (H_m), δ 6.34 (H_o) and δ 5.91 (H_l), as a result of the decreased exchange rate.

The combination of crown aromatic naphthalene and diimide aromatic proton upfield NMR shifts and their temperature dependence suggest **5** undergoes either an intramolecular or intermolecular crown–diimide complexation, with the diimide located inside the crown cavity. Unbound crown and diimide aromatics are undetectable at low temperature, suggesting the system associates quite strongly under such conditions. A NOESY experiment performed at 30 °C confirmed the suggested conformations, with correlations observed between the diimide protons (H_{a-d}) and both H_{18} and H_{24} on the crown. UV studies showed a charge transfer band at 484 nm, also indicative of the crown–diimide complexation.

Because of the flexible nature of the ethylene glycol subunits in **5** the diimide–crown complexation is most likely to be predominantly intramolecular. The self-association constant was calculated to be approximately 5.7† at −40 °C, indicating a relatively strong intramolecular interaction. Indeed, equating such an interaction to a typical intermolecular host–guest binding constant (for comparative purposes only) results in a value of 1140 M^{-1}‡ for an equivalent bimolecular process.

The intermolecular binding constant of an analogous rotaxane system, composed of **14** (the methyl ester of **9**), **2** and **3**, was calculated by NMR methods to be approximately 8.2 M^{-1} at −40 °C. This is an extremely weak binding constant for such a low temperature (*cf*. $K_a \approx 5000$ M^{-1} for the rotaxane system composed of **1**, **2** and **3** at the same temperature); thus any intermolecular interaction would be minimal under normal (mM) NMR concentrations of **5**.

The low temperature splitting of both diimide and crown naphthalene aromatic signals in the proton NMR spectrum of **5** suggest an unsymmetrical diimide–crown naphthalene interaction (Fig. 4a). This interaction is most likely an offset face-to-face π-interaction between both species, with H_l, H_m and H_n lying in more shielded positions over the naphthalene diimide π-bonding orbitals than H_o, H_p and H_q. Also, different diimide protons would experience different shielding effects depending on their position relative to the crown naphthalene aromatic. The depiction in Fig. 4a shows H_a in the most shielded position, followed by H_b, with H_c and H_d in less shielded positions. Each proton position can exchange with its partner, by the crown and diimide rocking back and forth and "yawing" from side to side (Fig. 4b).

The crown benzo aromatic protons (H_{i-k}) exhibit some interesting shifts at lower temperatures. H_i and H_j appear as one peak at 50 °C (δ 7.06), that splits into two at −50 °C (δ 7.12 and δ 6.80, respectively), while H_k appears as broad peak (δ 6.22) at 50 °C that shifts upfield dramatically on cooling to −50 °C (δ 4.70). The slight downfield shift for H_i and upfield shift for H_j, along with the very large upfield shift experienced by H_k, suggests an edge-to-face alignment of the benzo crown relative to the diimide aromatic, with H_k pointing directly at the diimide aromatic and the ethylene glycol linker units folding around the benzo sub-unit closer to H_j than H_l, as depicted in Fig. 5. Such a conformation of **5** also accounts for the slight deshielding effect experienced by H_i. In a 30 °C NOESY experiment, no NOEs were observed between H_j and the ethylene glycol linker protons, perhaps since H_j is closer to an oxygen than it is to any protons. However, a NOE was observed between H_k and H_{18}, consistent with an orientation of the crown benzo subunit pointing H_k into the crown cavity towards the complexed diimide, as predicted.

It might be expected that **5** could form higher-order oligomers in solution as well as the cyclic monomer [c1] conformation described. Indeed, there are some small peaks, visible in the proton NMR spectra of **5** at 30 °C, that show an aromatic spin-

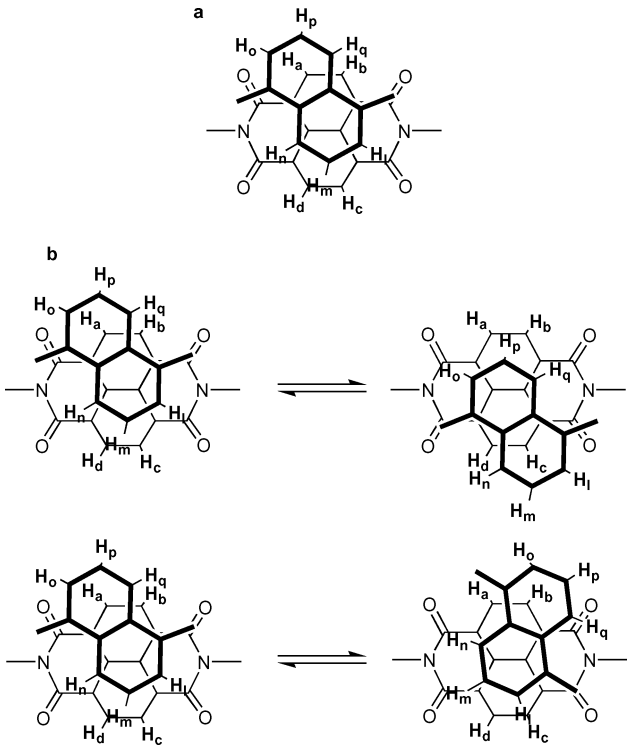

Fig. 4 (a) Exaggerated depiction of the offset face-to-face π-stacking between naphthalene crown (above) and naphthalene diimide (below) aromatics in **5**, as evidenced by low temperature NMR experiments; (b) some possible dynamic processes in the crown naphthalene–naphthalene diimide interaction include rocking back and forth (top) and "yawing" from side to side (below). Carbon–carbon double bonds and adjoining functional groups are omitted for clarity.

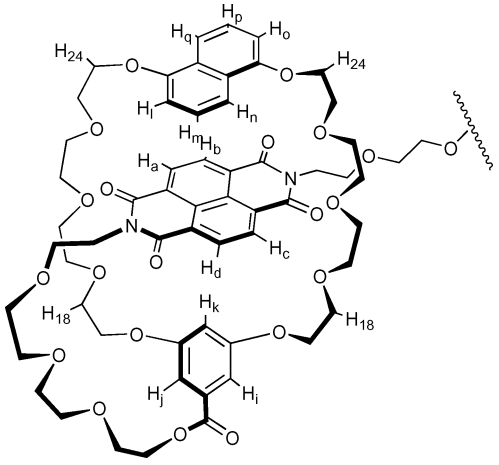

Fig. 5 The most dominant conformation of **5** at low temperature, as evidenced by ^{1}H NMR analysis, showing the edge-to-face interaction between the benzo crown aromatic and naphthalene diimide and the offset face-to-face interaction between the naphthalene crown aromatic and naphthalene diimide, as the diimide threads itself withing the crown cavity. The terminal pyridine and ethoxy groups are omitted for clarity.

system similar to that of the major [c1] conformer from COSY experiments. A DOSY experiment (see below) was performed on **5** at various temperatures, but was unable to detect the presence of any components larger than the [c1] monomer. It may be, however, that the small concentration of other possible co-conformers in our exchanging system is beyond the detectable limitations of such an experiment.

Addition of porphyrin **3** to the daisy chain component mixture (Scheme 1) was expected to stopper the system, effectively slowing down the exchange rate between daisy chain conformers and perhaps allowing observation of higher order oligomers. The terminal pyridyl group built into the structure of **5** enables

† The value is unitless as it pertains to the uncomplexed monomer ⇌ complexed monomer equilibrium.

‡ Value calculated by using host + guest ⇌ complex equilibrium for calculations, where [host] = [guest] = [uncomplexed monomer] and [complex] = [complexed monomer].

ruthenium–nitrogen coordination between the ruthenium porphyrin **3** and **5**.

Although the porphyrin was successful as a stopper component for the system, the exchange rate between intramolecularly diimide-complexed [c1] and uncomplexed [a1] daisy chain monomers was only slowed slightly on stoppering. Low temperature NMR experiments showed distinguishable peaks for the bound and unbound crown and diimide protons only at temperatures below −30 °C, compared to the parent rotaxane system **4** (a mixture of **1**, **2** and **3**), that showed similarly distinguishable peaks at room temperature.[7] Perhaps this result is indicative of the inherently fast intramolecular exchange process present in the mixture of **5** and **3**, compared to the slower intermolecular exchange in the mixture of **1**, **2** and **3**.

Further NMR analysis of the mixture of **5** and **3**, including DOSY and COSY techniques, showed similar results to the study of the unstoppered system. That is, stoppering the daisy chain system **5** does not observably effect the distribution of co-conformer products. Indeed, the major product co-conformer formed by mixing **5** and **3** in chloroform was the [c1] self-complexing, porphyrin-stoppered monomer **7**. Higher order daisy chain oligomers were undetectable under these conditions.§

Thread-porphyrin hybrid. The structural conformation of **6** in solution was obtained primarily using similar NMR techniques. Scheme 2 shows the non-systematic numbering system used to compare the target compound **6** with its free-base **16** and mono-functional thread **11** precursors.

Dramatic and informative chemical shift differences were observed between **6** and its precursors, the free-base **16** and monofunctional thread **11** (Fig. 6). A downfield shift was observed for H_{16} in the free-base compound **16** (δ 4.29), compared to its precursor **11** (δ 3.64), indicative of its location close to the subunit fusing ester group in **16**. More importantly, the free-base compound **16** also showed significant upfield shifts for the diimide protons, H_{a-d} (from δ 8.76 in **11** to δ 7.20 in **16**), and their nearest ethylene glycol neighbour protons, $H_{8,9}$ (from δ 4.48 in **11** to δ 4.03 in **16**) and $H_{7,10}$ (from δ 3.86 in **11** to δ 3.46 in **16**), when compared to the corresponding monofunctional thread **11** protons. These shifts are indicative of a face-to-face porphyrin–diimide intramolecular interaction in **16** (Fig. 7), where the diimide and neighbouring protons lie above the porphyrin subunit, and are heavily shielded as a result.[7,10]

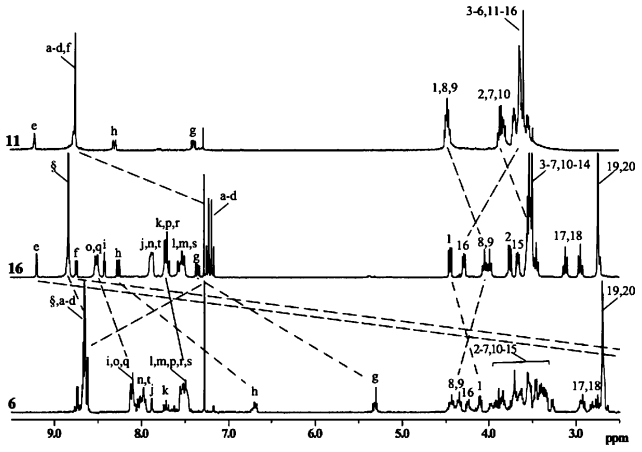

Fig. 6 ^{1}H NMR comparison of target compound **6** (bottom) and its precursors **11** (top) and **16** (middle) at 30 °C in $CDCl_3$. Significant chemical shift differences are highlighted with dotted lines.

§ Although the CSI-MS spectra show evidence of traces of higher order oligomers, these would amount to <5%, assuming approximate linear response in the mass spectral technique. Such minor quantities would be hardly detectable in the NMR spectra and, in any case, could well be masked by the larger monomer peaks.

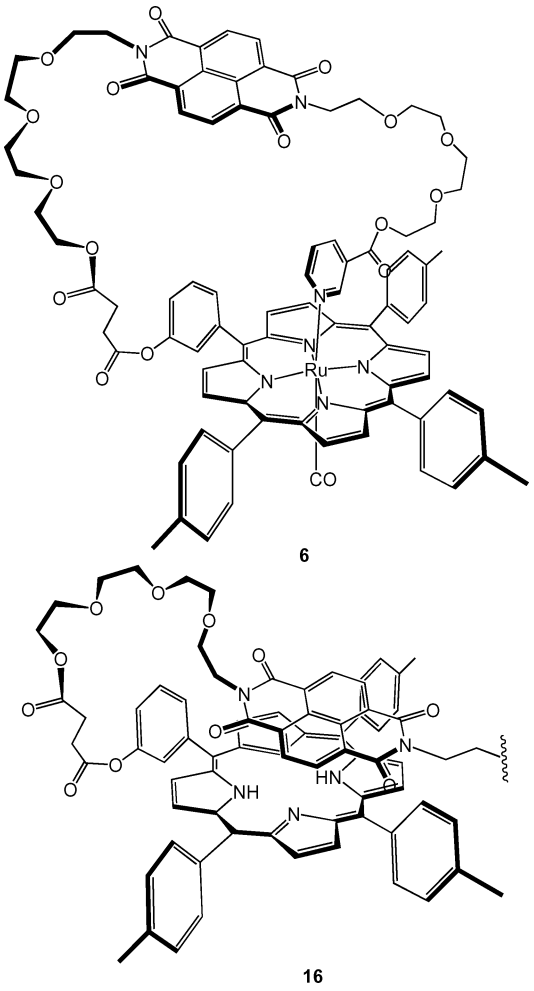

Fig. 7 Depiction of the porphyrin–diimide intramolecular folding effect in **16** (top) and the intramolecular pyridyl–ruthenium coordination in **6** (bottom). Terminal ethylene glycol and pyridyl groups are omitted for clarity in the depiction of **16**.

In the target compound **6**, the terminal pyridine is now directly coordinated to a ruthenium porphyrin and hence their protons H_e, H_f, H_g and H_h are greatly shifted upfield when compared to the corresponding free-base **16** protons. H_e and H_f, the protons closest to the pyridyl nitrogen are shifted the furthest, from δ 9.20 to δ 2.15 and from δ 8.75 to δ 1.65, respectively, while H_g and H_h shift upfield from δ 8.25 to δ 6.69 and from δ 7.38 to δ 5.31, respectively. The closest proton H_1 to the pyridine subunit is also shifted upfield from δ 4.45 in **16** to δ 4.11 in **6**. These shifts are indicative of either an intra- or inter-molecular ruthenium–pyridyl coordination process (Fig. 7), leaving the terminal pyridine heavily shielded by the porphyrin macrocycle. The diimide protons, H_{a-d}, shift downfield from δ 7.20 in **16** to their more normal position δ 8.65 in **6**, as do the diimide adjacent protons $H_{8,9}$ (from δ 4.03 in **16** to δ 4.37 in **6**), as the pyridyl–ruthenium coordination on one side of the porphyrin and the carbonyl ligand on the other now prevent any porphyrin–diimide interaction from occurring. The porphyrin tolyl aromatic peaks reflect the lack of symmetry between each porphyrin face in **6**, appearing at δ 7.98 ($H_{n,t}$) and δ 7.52 ($H_{m,s}$) for the pyridine coordinated face and δ 8.11 ($H_{o,q}$) and δ 7.52 ($H_{p,r}$) for the carbonyl ligand face. Table 1 summarises and compares the aromatic and aromatic adjacent proton shifts between **6** and **16**.

It was predicted that the potentially self-coordinating thread-porphyrin fused compound **6** could be utilised to form a [2]catenane **8** by simply incorporating a dinaphthalene-38-crown-10 **1** component in solution, according to Scheme 2. The ease of synthesis highlights the advantage of such a self-assembly process. The non-systematic labelling system shown in Scheme 2 was used for the ^{1}H NMR study of the mixture of **6** and **1** in solution.

Table 1 ^{1}H NMR data ($CDCl_3$ at 30 °C) for aromatic and aromatic adjacent protons of **16** and **6**, highlighting significant shifts due to pyridyl–ruthenium coordination in **6** (*italics*) and diimide–porphyrin complexation in **16** (*bold*)

Proton	**16** (ppm)	**6** (ppm)	$\Delta\delta$
a–d	7.20	8.65	**+1.45**
e	9.20	2.15	*−7.05*
f	8.75	1.65	*−7.10*
g	8.25	6.69	*−1.56*
h	7.38	5.31	*−2.07*
i	8.45	7.89	−0.56
j	7.85	8.11	+0.26
k	7.69	7.72	+0.03
l	7.58	7.52	−0.06
m	7.52	7.52	0.00
n	7.85	7.98	+0.13

COSY NMR measurements proved extremely useful in studying the solution mixture of **6** and **1** (Fig. 8). Obvious aromatic shifts and spin systems are apparent for the terminal pyridine (H_{e-h}), diimide (H_{a-d}) and porphyrin ($H_{i-t,\beta}$) protons in **6** and the naphthalene crown (H_{u-w}) aromatics in **1**. Of particular interest are the presence of both unbound and bound crown (δ 7.79, δ 7.19, δ 6.53 (H_{u-w} unbound) and δ 6.77, δ 6.62 and δ 6.06 (H_{u-w} bound)) and diimide (δ 8.72 (H_{a-d} unbound) and δ 8.15 (H_{a-d} bound)) protons, indicative of both a slow exchange process between the species, due to the intramolecular porphyrin coordination *clipping* effect, and the presence of [2]catenane **8**.

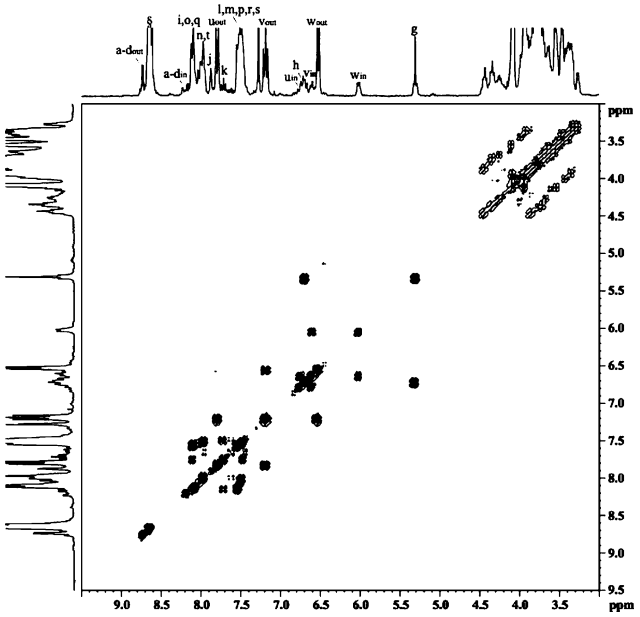

Fig. 8 COSY NMR of **6** and **1** mixed in $CDCl_3$ at 30 °C. Aromatic peaks are labelled according to Scheme 2. *In* and *out* labelling designate crown–diimide species complexed and uncomplexed, respectively.

The system exhibited a binding constant estimated from single point analysis to be 140 M^{-1} at 273 K and a curved van't Hoff plot (Fig. 9)¶. Of course, in the [2]catenane **8** mixture, the folding nature of the porphyrin coordination ring-closing mechanism, required for catenation, along with the possibility of intermolecular porphyrin–pyridine coordination are events that likely interfere with the crown–diimide interaction, yielding a non-zero heat capacity term (ΔC_p) characterised by a non-linearity in the van't Hoff plot. These events are prohibited in the analogous parent self-assembling porphyrin-stoppered rotaxane system **4**, which yields a linear van't Hoff plot.[7]

¶ We have observed non-linear van't Hoff plots previously in pseudorotaxane systems and they are indicative of a non-zero heat capacity term (ΔC_p).[7]

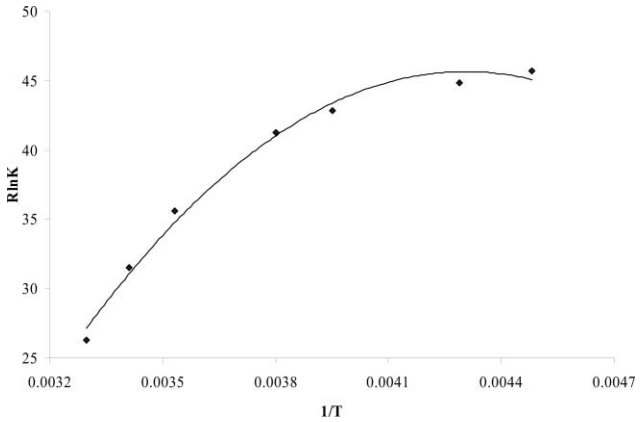

Fig. 9 Van't Hoff plot for the mixture of **1** and **6** in $CDCl_3$.

There is the possibility of intermolecular coordination occurring in **6**, affording higher order oligomers with the opportunity to form [3]catenane and higher interlocked super-structures upon the inclusion of **1**. This possibility was investigated using DOSY NMR (Fig. 10), a useful technique for analysing mixtures of compounds of widely varying sizes.[11] The experiment showed the presence of only two differently sized species, presumably the [2]catenane **8** and uncomplexed crown **1** from the mixture of **6** and **1**, in $CDCl_3$. It is expected that uncomplexed **6** would be present in the mixture, but since it would have a similar molecular size to **8**, with overlapping chemical shifts, it would be impossible to identify using the 2D DOSY technique under these measurement conditions. No higher-order oligomers were observed.* NMR experiments were performed on **6** at various concentrations to observe any spectral changes caused by intermolecular complexation that was expected to be favoured at higher concentrations. However, no significant changes were seen over the concentrations (0.25 mM to 31.6 mM) used. Higher concentrations were unattainable due to the poor solubility of the compound. Similar to the daisy chain **7**, which contains an equally flexible structure, these results are consistent with **8** being most stable in its monomeric state under our experimental conditions.

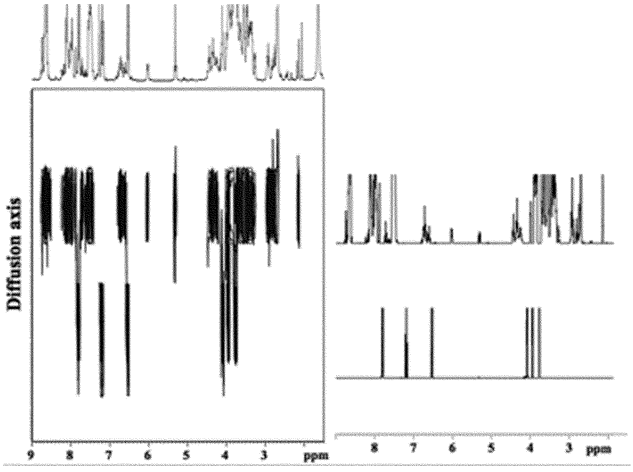

Fig. 10 DOSY NMR experiment (left) performed on the mixture of **6** and **1** in $CDCl_3$ at 30 °C (0.01 M). The presence of components **8** (above) and **1** (below) are evident. Their corresponding 1D proton NMR slices are shown on the right. Component **6** is expected to be present in the mix, but overlaps with **8** on the diffusion axis.

CSI-MS analysis. Cold spray ionisation mass spectrometry (CSI-MS) is a technique in its infancy. Developed by Yamaguchi and coworkers[12] to characterise labile organometallic

* This result does not infer that no higher oligomers are present; only that if they are present, they are at such low concentrations with similar chemical shifts compared to the [2]catenane **8** that they are undetectable in our experiment.

compounds, it utilises the higher dielectric constant of many solvents at lower temperatures, to afford low temperature ionisation by solvation. This low temperature (−50 to 15 °C) ionisation allows thermally unstable ions to reach the mass analyser without decomposition. Yamaguchi *et al.*[13] have used CSI-MS to prove the formation of a [3]catenane from twelve components in solution, based upon the interaction between palladium and nitrogen ligands. The [3]catenane molecular ion was unobservable using normal electrospray ionisation or fast atom bombardment MS techniques.

Likewise, conventional MS techniques on both our stoppered daisy chain and catenane systems in solution show only peaks corresponding to individual component masses and none of the expected supramolecular complex molecular ion peaks corresponding to the formation of **7** and **8**, because the ionisation techniques are too energetic for the labile products. However, the CSI-MS technique on these systems proved very successful.

When the mixture of **5** and **3** in $CHCl_3$ was analysed using CSI-MS, peaks were observed for the daisy chain monomer **5**, porphyrin stopper **3**, stoppered daisy chain monomer **7**, mono-stoppered daisy chain dimer **17** and di-stoppered daisy chain dimer **15** (Fig. 11). The relative peak sizes confirm the predominant intramolecular complexation expected in **5**.

When CSI-MS was performed on the mixture of **6** and **1** in $CHCl_3$, the spectrum showed the presence of the crown **1**, thread-fused porphyrin **6**, [2]catenane **8** and thread-fused porphyrin dimer **18** (Fig. 12). Formation of the thread-fused dimer **18** involves intermolecular porphyrin–pyridine coordination, although this appears to be a minor product in the mixture, confirming the expected preference for **6** to adopt an intramolecular porphyrin–pyridine coordination co-confomation.

These results appear to confirm the co-conformations predicted from the NMR data. However, the mild ionisation process involved in the CSI-MS technique limits the unequivocal characterisation of target molecular ions, since non-specific associated components with masses indistinguishable from the target products might also be detectable using the technique. CSI-MS is nonetheless a useful tool, when used in conjunction with other techniques, to analyse these types of labile systems.

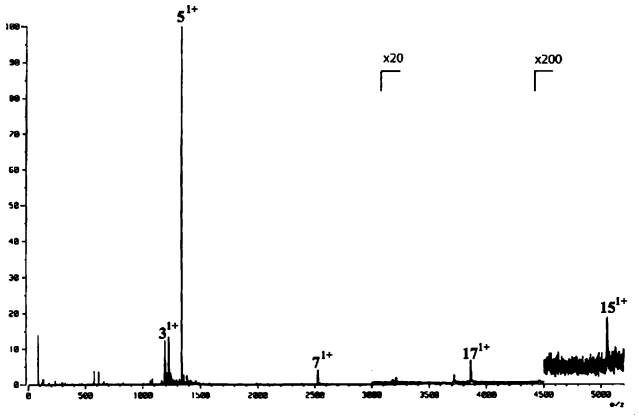

Fig. 11 CSI-MS for the mixture of **5** and **3** in $CHCl_3$ shows the presence of porphyrin **3**, daisy chain monomer **5**, stoppered daisy chain monomer **7**, mono-stoppered daisy chain dimer **17** and di-stoppered daisy chain dimer **15**.

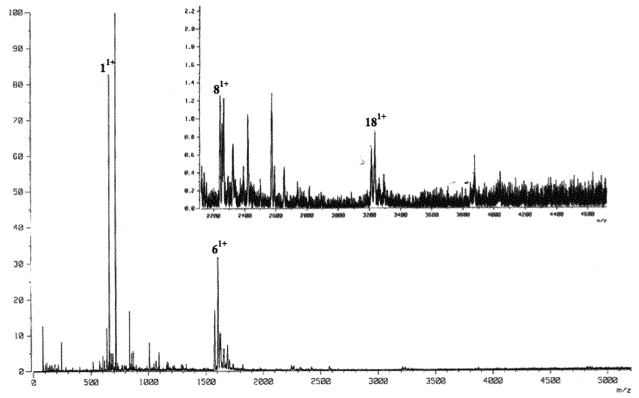

Fig. 12 CSI-MS for the mixture of **6** and **1** in $CHCl_3$. The region from 2100–4700 m/z is expanded and shown inset (upper-right). Peaks corresponding to the crown **1**, thread-fused porphyrin **6**, [2]catenane **8** and thread-fused porphyrin dimer **18** can be observed.

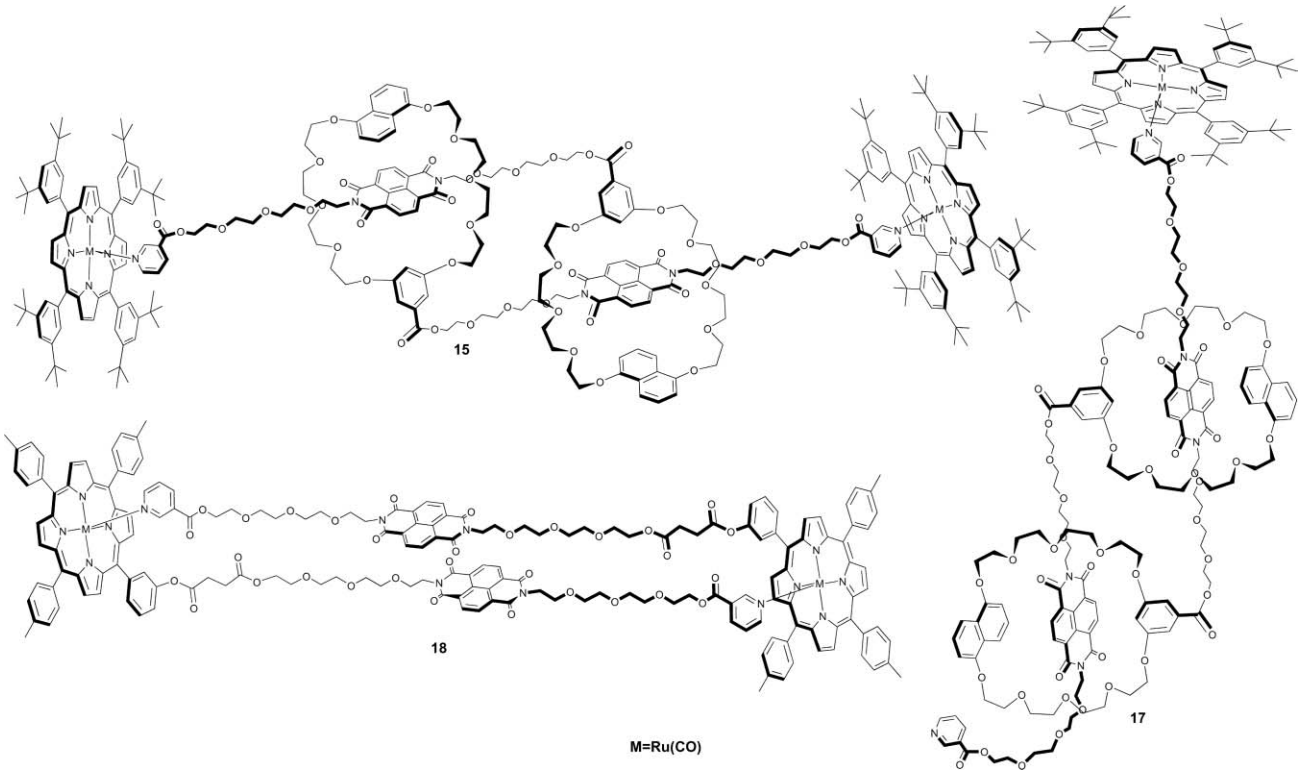

Conclusions

A series of self-assembling rotaxane component hybrid systems, of varying complexity, have been successfully constructed and analysed, primarily using various NMR techniques. With relatively simple synthetic routes but interesting properties, they provide an insight into the types of systems that in the future might form the basis of switching devices for nano-sized products. Indeed, the simple, reversible assembly process associated with such supramolecular systems allow quite large, complex, multi-functional targets to be formed simply by mixing suitably designed components under controlled conditions.

Although the synthesis of both the crown-thread **5** and porphyrin-thread **6** hybrid species were relatively straightforward, determining the co-conformer composition in solution proved more complicated. 2D NMR techniques, including DOSY NMR, proved useful in characterising the systems, but each had their limitations.

Ultimately, it can be concluded that under the experimental conditions (0.034 M in $CDCl_3$), the primary co-conformer products when **5** is dissolved in a suitable solvent are the [c1] and [a1] monomers, although there is limited evidence to suggest the presence in low concentrations of higher order co-conformers. Likewise, **6** seems to prefer a monomeric co-conformation under similar experimental conditions.

Addition of **3** to the monomer **5** in solution successfully stoppered the daisy chain system and enabled CSI-MS analysis, which showed a low percentage of higher-order oligomers in the resulting mixture. Addition of **1** to **6** in solution yielded the target [2]catenane **8**. Its formation was evidenced through COSY and DOSY NMR experiments. CSI-MS analysis confirmed the predominance of **8** in solution, but also the presence of higher oligomeric co-conformations in low concentrations. These results highlight the complexity of such multi-functional component mixtures in solution.

Modification of both **5** and **6**, by both incorporation of shorter[14] or more rigid[15] linker subunits and the use of stronger binding components, could afford supramolecular mixtures with a larger percentage of higher-order co-conformers. This would prove useful as the basis for larger, complex superstructures. However, primarily self-complexing monomeric structures such as **5** and **6** could represent a useful improvement to established supramolecular switching devices. Many such devices involve the expulsion of one component from the other, followed by the self-assembling recombination of both components from a solution mixture. Clearly both **5** and **6**, once suitably modified, could be used for similar switching processes, having the advantage of keeping the expelled component in close proximity. This would permit rapid recombination and ultimately afford faster switching devices.

Experimental

2-[2-(2-{2-[2-Nicotinoyloxyethoxy]ethoxy}ethoxy)ethyl]-7-[2-(2-{2-[2-({1,5-naptho}-35-crown-10-{1,3-dioxybenzene-5-carboxyl})ethoxy]ethoxy}ethoxy) ethyl]benzo[lmn]-[3,8]phenanthroline-1,3,6,8-tetraone (5)

1(1,5)-Naphthalena 15(1,3)-(5-carboxybenzena)-2,5,8,11,14,16,19,22,25,28-decaoxacyclo-octacosaphane **9** (37.1 mg, 58.86 μmol),[16] 2-[2-(2-{2-[2-nicotinoyloxyethoxy]ethoxy}-ethoxy)ethyl],7-[2-(2-{2-[2-hydroxyethoxy]ethoxy}ethoxy) ethyl]benzo[lmn]-[3,8]phenanthroline-1,3,6,8-tetraone **11** (42.6 mg, 58.86 μmol), HOBT (16.0 mg, 117.72 μmol) and EDC (17.0 mg, 88.29 μmol) were dissolved in a mixture of THF (3.0 mL) and chloroform (3.0 mL) in a 10 mL round bottomed flask under nitrogen. The resulting red solution was stirred at rt. Triethylamine (6.0 mg, 8.3 μL, 58.86 μmol) was added *via* a syringe and the solution was stirred for 2 days. Then the solvent was evaporated and the red oil crude product was taken up in 6 M HCl and diethyl ether. The aqueous layer was separated and neutralised with sat. $NaHCO_3$, then extracted with chloroform (4 × 50 mL), dried over sodium sulfate and the solvent evaporated. The product was isolated by preparative TLC (SiO_2: 10% MeOH–DCM) as a red oil (R_f = 0.654) (33.4 mg, 24.99 μmol, 43%); *m/z* (ES-MS) $[M + H]^+$ 1336.5337 $C_{69}H_{82}N_3O_{24}$ (calc. 1336.5288); ^{1}H NMR (300 MHz, $CDCl_3$) δ 9.22 (1H, d, Ar–H), 8.75 (1H, dd, Ar–H), 8.65 (4H, s, Ar–H), 8.30 (1H, m, Ar–H), 7.55 (2H, dd, Ar–H), 7.38 (1H, m, Ar–H), 7.11 (2H, t, Ar–H), 7.02 (2H, d, Ar–H), 6.58 (2H, dd, Ar–H), 5.99 (1H, br s, Ar–H), 4.49 (2H, t, OCH_2), 4.42 (4H, t, OCH_2), 4.28 (2H, t, OCH_2), 4.15 (4H, t, OCH_2), 3.97 (4H, t, OCH_2), 3.82 (12 H, m, OCH_2), 3.77 (4H, m, OCH_2), 3.72 (16H, m, OCH_2), 3.67 (16H, m, OCH_2); ^{13}C NMR (75 MHz, $CDCl_3$) δ 166.1 (C=O), 165.2 (C=O), 162.7 (C=O), 159.5 (Ar), 153.9 (Ar), 153.6 (Ar), 153.3 (Ar), 151.0 (Ar), 137.1 (Ar), 131.6 (Ar), 131.1 (Ar), 126.0 (Ar), 124.7 (Ar), 123.2 (Ar), 114.4 (Ar), 107.8 (Ar), 105.8 (Ar), 105.2 (Ar), 71.1, 70.9, 70.8, 70.7, 70.1, 69.8, 69.4, 69.1, 67.9, 67.5, 64.2, 53.4, 39.5, 29.7, 14.2; UV (λ nm (ε/dm^3 mol^{-1} cm^{-1}), CH_2Cl_2) 484 (3.44 × 10^2).

2-[2-(2-{2-[2-Nicotinoyloxyethoxy]ethoxy}ethoxy)ethyl]-7-[2-(2-{2-[2-(3-{ruthenium carbonyl 5-[phen-3-yl]10,15,20-*tris*-[*p*-tolyl] porphyrinyl}carboxypropionyloxy) ethoxy]ethoxy}ethoxy)-ethyl]benzo[lmn]-[3,8]phenanthroline-1,3,6,8-tetraone (6)

2-[2-(2-{2-[2-Nicotinoyloxyethoxy]ethoxy}ethoxy)ethyl]-7-[2-(2-{2-[2-(3-{5-[phen-3-yl]10,15,20-*tris*-[*p*-tolyl] porphyrinyl}carboxypropionyloxy)ethoxy]ethoxy}ethoxy)ethyl]benzo[lmn]-[3,8]-phenanthroline-1,3,6,8-tetraone **16** (371 mg, 251 μmol) was dissolved in dry toluene (80 mL). Triruthenium dodecacarbonyl (400 mg, 626 μmol) was subsequently added. The mixture was freeze–pump–thawed and then refluxed under nitrogen in the dark for 2 days, before being cooled to rt and filtered through a celite plug. Column chromatography (SiO_2: 10% hexane–DCM to DCM to 2% MeOH–DCM, followed by another column with DCM to 1% MeOH–DCM) yielded 207.8 mg of the pure red solid product (52%), mp 146–148 °C; *m/z* (ES-MS) $[M + Na]^+$ 1628.435 $Ru_1C_{88}H_{77}N_7O_{17}Na_1$ (calc. 1628.431); ^{1}H NMR (300 MHz, $CDCl_3$) δ 8.65 (8H, m, β-H), 8.65 (4H, s, Ar–H), 8.11 (3H, d, Ar–H), 8.11 (1H, s, Ar–H), 7.99 (3H, d, Ar–H), 7.88 (1H, dd, Ar–H), 7.72 (1H, dd, Ar–H), 7.53 (6H, m, Ar–H), 7.53 (1H, dd, Ar–H), 6.69 (1H, m, py-H), 5.31 (1H, m, py-H), 4.43 (2H, m, OCH_2), 4.35 (2H, m, OCH_2), 4.24 (2H, m, OCH_2), 4.11 (2H, m, OCH_2), 3.96–3.84 (4H, m, OCH_2), 3.71–3.54 (10H, m, OCH_2), 3.47–3.29 (10H, m, OCH_2), 2.94 (2H, t, CH_2), 2.75 (2H, t, CH_2), 2.70 (9H, s, Ar–CH_3), 2.15 (1H, s, py-H), 1.65 (1H, m, py-H); ^{13}C NMR (75 MHz, $CDCl_3$) δ 180.3, 172.0, 171.0, 162.8, 162.4, 162.2, 159.8, 149.1, 148.9, 147.5, 145.8, 144.1, 143.9, 143.8, 143.3, 139.6, 136.8, 135.3, 134.2, 134.0, 132.5, 132.1, 131.8, 131.5, 131.0, 130.9, 128.8, 128.5, 128.0, 127.6, 127.3, 127.0, 126.7, 126.6, 124.1, 121.9, 121.7, 121.2, 120.4, 120.3, 119.8, 108.1, 70.93, 70.86, 70.62, 70.50, 70.43, 70.29, 70.10, 70.03, 69.59, 69.00, 68.88, 68.47, 67.82, 67.71, 63.95, 63.82, 39.55, 29.70, 29.32, 29.19, 28.96, 21.50, 14.11; UV (λ nm (ε/dm^3 mol^{-1} cm^{-1}), CH_2Cl_2) 412 (2.34 × 10^5), 533 (2.03 × 10^4), 566 (6.69 × 10^3).

2-[2-(2-{2-[2-Nicotinoyloxyethoxy]ethoxy}ethoxy)ethyl]-7-[2-(2-{2-[2-hydroxyethoxy]ethoxy}ethoxy)ethyl]benzo[lmn]-[3,8]phenanthroline-1,3,6,8-tetraone (11)

2,7-Bis-[2-(2-{2-[2-hydroxyethoxy]ethoxy}ethoxy)ethyl]benzo[lmn]-[3,8]phenanthroline-1,3,6,8-tetraone **10**[17] (50.0 mg, 81 μmol), nicotinic acid (10.0 mg, 81 μmol), HOBT (22.0 mg, 162 μmol) and EDC (23.3 mg, 121.5 μmol) were dissolved in a mixture of THF (2.0 mL) and chloroform (2.0 mL) in a 10 mL round bottomed flask. Triethylamine (8.2 mg, 11.3 μL, 81 μmol) was added *via* a syringe and the solution was stirred at rt under nitrogen in the dark for 2 days. The solvent was evaporated and the residue was taken up in 6 M HCl and chloroform. The aqueous layer was separated and neutralised with sat.

$NaHCO_3$. The product was extracted with chloroform, dried over Na_2SO_4 and the solvent removed using a rotary evaporator to yield a yellow–brown oil which was subjected to preparative TLC (SiO_2, 8% MeOH–$CHCl_3$). The product was obtained as a yellow oil (19 mg, 33%); *m/z* (EI-MS) $[M]^+$ 723.2627 $C_{36}H_{41}N_3O_{13}$ (calc. 723.2639); ^{1}H NMR (300 MHz, $CDCl_3$) δ 9.22 (1H, d, Ar–H), 8.76 (4H, s, Ar–H), 8.76 (1H, dd, Ar–H), 8.30 (1H, dd, Ar–H), 7.39 (1H, dd, Ar–H), 4.48 (6H, m, OCH_2), 3.84 (6H, m, OCH_2), 3.54–3.73 (20H, m, OCH_2); ^{13}C NMR (75 MHz, $CDCl_3$) δ 165.2, 162.9, 153.4, 151.0, 137.1, 130.9, 126.8, 126.7, 126.6, 126.0, 123.2, 72.5, 70.7, 70.6, 70.3, 70.1, 69.0, 67.8, 64.5, 61.7, 39.6.

5-[*m*-Hydroxyphenyl]10,15,20-*tris*-[*p*-tolyl] porphyrin (12)

A solution of 3-hydroxybenzaldehyde (4 g, 33 mmol) in propionic acid (200 mL) was warmed to 120 °C with vigorous stirring. 4-Tolualdehyde (7.7 mL, 66 mmol) then pyrrole (6.8 mL, 99 mmol) were added and the mixture was refluxed vigorously for 1 h in air. The solution was cooled to rt and the precipitate filtered off, washed with ethanol and dried. The resulting porphyrin mixture was subjected to column chromatography (SiO_2: DCM) to yield 739 mg of the pure purple porphyrin product (3.3%), mp > 320 °C; *m/z* (ES-MS) $[M + H]^+$ 673.2971 $C_{47}H_{37}N_4O$ (calc. 673.2967); ^{1}H NMR (300 MHz, $CDCl_3$) δ 8.87 (8H, d, β-H), 8.11 (6H, d, Ar–H), 7.81 (1H, dd, Ar–H), 7.71 (1H, s, Ar–H), 7.62 (1H, t, Ar–H), 7.57 (6H, d, Ar–H), 7.28 (1H, dd, Ar–H), 2.73 (9H, s, CH_3), −2.74 (2H, broad-s, NH); ^{13}C NMR (75 MHz, $CDCl_3$) δ 139.3, 137.3, 134.5, 131.1, 130.9, 127.7, 127.4, 21.5; UV(λ nm (ε/dm^3 mol^{-1} cm^{-1}), CH_2Cl_2) 419 (4.22×10^5), 515 (1.77×10^4), 550 (8.89×10^3), 590 (5.55×10^3), 647 (5.89×10^3).

5-[3-(3-Carboxypropionyloxy)phenyl]10,15,20-*tris*-[*p*-tolyl] porphyrin (13)

5-[*m*-Hydroxyphenyl]10,15,20-*tris*-[*p*-tolyl] porphyrin **12** (1.0 g, 1.4786 mmol) was dissolved in dry DCM (50 mL). NEt_3 (225.3 mg, 0.310 mL, 2.230 mmol) was added *via* a syringe, followed by succinic anhydride (223 mg, 2.230 mmol) and DMAP (181.6 mg, 1.486 mmol). The solution was stirred at rt under nitrogen in the dark for 7 days. Then the solvent was evaporated and the residue was taken up in a mixture of chloroform and water. The organic layer was separated and dried (Na_2SO_4) before the solvent was evaporated and the residue purified by column chromatography (SiO_2: DCM to 1% MeOH–DCM) yielding 840 mg of the purple solid product (73%), mp 141–143 °C; *m/z* (ES-MS) $[M + H]^+$ 773.3121 $C_{51}H_{41}N_4O_4$ (calc. 773.3128); ^{1}H NMR (300 MHz, $CDCl_3$) δ 8.87 (8H, d, β-H), 8.11 (6H, d, Ar–H), 8.09 (1H, dd, Ar–H), 7.98 (1H, s, Ar–H), 7.74 (1H, t, Ar–H), 7.56 (6H, d, Ar–H), 7.55 (1H, dd, Ar–H), 2.95 (2H, t, CH_2), 2.84 (2H, t, CH_2), 2.72 (9H, s, CH_3), −2.72 (2H, broad-s, NH); ^{13}C NMR (75 MHz, $CDCl_3$) δ 176.1, 170.9, 149.1, 147.2, 146.6, 143.7, 139.2, 137.4, 134.5, 134.0, 132.3, 131.7, 131.2, 129.2, 128.5, 127.7, 127.4, 120.8, 120.5, 120.3, 118.2, 113.2, 85.0, 29.7, 29.2, 28.7, 23.9, 22.7, 21.5, 17.3, 17.1; UV (λ nm (ε/dm^3 mol^{-1} cm^{-1}), CH_2Cl_2) 418 (2.26×10^5), 515 (1.05×10^4), 551 (5.90×10^3), 590 (4.12×10^3), 645 (3.68×10^3).

2-[2-(2-{2-[2-Nicotinoyloxyethoxy]ethoxy}ethoxy)ethyl]-7-[2-(2-{2-[2-(3-{5-[phen-3-yl]10,15,20-*tris*-[*p*-tolyl] porphyrinyl}-carboxypropionyloxy) ethoxy]ethoxy}ethoxy)ethyl]benzo[lmn]-[3,8]phenanthroline-1,3,6,8-tetraone (16)

2-[2-(2-{2-[2-Nicotinoyloxyethoxy]ethoxy}ethoxy)ethyl]-7-[2-(2-{2-[2-hydroxyethoxy]ethoxy}ethoxy)ethyl]benzo[lmn]-[3,8]-phenanthroline-1,3,6,8-tetraone **11** (500.03 mg, 692 μmol), 5-[3-(3-carboxy-propionyloxy)-phenyl]10,15,20-*tris*-[*p*-tolyl] porphyrin **13** (535 mg, 692 μmol), HOBT (135.1 mg, 1.0 mmol) and EDC (332 mg, 1.73 mmol) were dissolved in DCM (25 mL). Triethylamine (101 mg, 1.0 mmol) was added *via* a syringe and the mixture was stirred at rt under nitrogen in the dark for 3 days. The solvent was removed and the mixture subjected to column chromatography (SiO_2: DCM to 2% MeOH–DCM) to afford 520.6 mg of the product as a purple solid (51%), mp 79–82 °C; *m/z* (ES-MS) $[M + H]^+$ 1478.5686 $C_{87}H_{80}N_7O_{16}$ (calc. 1478.5662); ^{1}H NMR (300 MHz, $CDCl_3$) δ 9.21 (1H, s, Ar–H), 8.84 (8H, s, Ar–H), 8.75 (1H, dd, Ar–H), 8.51 (3H, dd, Ar–H), 8.42 (1H, s, Ar–H), 8.25 (1H, dd, Ar–H), 7.88 (3H, m, Ar–H), 7.88 (1H, dd, Ar–H), 7.71 (3H, dd, Ar–H), 7.68 (1H, dd, Ar–H), 7.58 (1H, dd, Ar–H), 7.53 (3H, dd, Ar–H), 7.35 (1H, dd, Ar–H), 7.21 (4H, q, Ar–H), 4.45 (2H, m, OCH_2), 4.29 (2H, m, OCH_2), 4.05 (2H, m, OCH_2), 3.99 (2H, m, OCH_2), 3.76 (2H, m, OCH_2), 3.67 (2H, m, OCH_2), 3.46–3.56 (20H, m, OCH_2), 3.11 (2H, t, OCH_2), 2.96 (2H, m, OCH_2), 2.73 (9H, s, tol-H), −3.89 (2H, s, NH); ^{13}C NMR (75 MHz, $CDCl_3$) δ 172.0, 171.2, 161.3, 161.1, 153.4, 151.0, 149.4, 143.4, 139.1, 139.0, 137.4, 137.1, 135.1, 134.1, 132.6, 131.1, 128.0, 127.8, 127.6, 127.4, 123.6, 123.2, 120.7, 120.4, 120.2, 118.0, 70.9, 70.7, 70.6, 70.5, 70.3, 70.0, 69.9, 69.0, 68.9, 67.6, 67.4, 64.4, 63.9, 39.2, 29.7, 29.4, 21.5; UV (λ nm (ε/dm^3 mol^{-1} cm^{-1}), CH_2Cl_2) 420 (1.01×10^5), 516 (9.56×10^3), 551 (6.21×10^4), 592 (4.34×10^3), 648 (4.34×10^3).

Acknowledgements

We thank Dr David Tucker, University of New England, for help with the DOSY NMR experiments and Mr Yoshihisa Sei, Faculty of Pharmaceutical Sciences at Kabawa Campus, Tokushima Bunri University for assistance with the CSI-MS measurements. We acknowledge funding support from the Australian Research Council.

References

1 G. J. E. Davidson, S. J. Loeb, N. A. Parekh and J. A. Wisner, *J. Chem. Soc., Dalton Trans.*, 2001, 3135; X. Zhao, X.-K. Jiang, M. Shi, Y.-H. Yu, W. Xia and Z.-T. Li, *J. Org. Chem.*, 2001, **66**, 7035; F. G. Gatti, D. A. Leigh, S. A. Nepogodiev, A. M. Z. Slawin, S. J. Teat and J. K. Y. Wong, *J. Am. Chem. Soc.*, 2001, **123**, 5983; D. Tuncel and J. H. G. Steinke, *Chem. Commun.*, 2002, 496; P. Gavina and J.-P. Sauvage, *Tetrahedron Lett.*, 1997, **38**, 3521; J.-C. Chambron and J.-P. Sauvage, *Chem. Eur. J.*, 1998, **4**, 1362; J.-P. Collin, P. Gavina and J.-P. Sauvage, *New J. Chem.*, 1997, **21**, 525.

2 A. C. Try, M. M. Harding, D. G. Hamilton and J. K. M. Sanders, *Chem. Commun.*, 1998, 723; C. P. McArdle, M. C. Jennings, J. J. Vittal and R. J. Puddephatt, *Chem. Eur. J.*, 2001, **7**, 3572; G. Hungerford, M. Van der Auweraer and D. B. Amabilino, *J. Porphyrins Phthalocyanines*, 2001, **5**, 633; D. A. Leigh, P. J. Lusby, S. J. Teat, A. J. Wilson and J. K. Y. Wong, *Angew. Chem., Int. Ed.*, 2001, **40**, 1538; P. R. Ashton, R. Ballardini, V. Balzani, M. Gomez-Lopez, S. E. Lawrence, M. V. Martinez-Diaz, M. Montalti, A. Piersanti, L. Prodi, J. F. Stoddart and D. J. Williams, *J. Am. Chem. Soc.*, 1997, **119**, 10641; P. R. Ashton, V. Baldoni, V. Balzani, A. Credi, H. D. A. Hoffmann, M.-V. M. Diaz, F. M. Raymo, J. F. Stoddart and M. Venturi, *Chem. Eur. J.*, 2001, **7**, 3482; A. Credi, M. Montalti, V. Balzani, S. J. Langford, F. M. Raymo and J. F. Stoddart, *New J. Chem.*, 1998, 1061; M. J. Gunter, S. M. Farquhar and T. P. Jeynes, *Org. Biomol. Chem.*, 2003, **1**, 4097; M. J. Gunter and S. M. Farquhar, *Org. Biomol. Chem.*, 2003, **1**, 3450; M. J. Gunter, D. C. R. Hockless, M. R. Johnston, B. W. Skelton and A. H. White, *J. Am. Chem. Soc.*, 1994, **116**, 4810; M. J. Gunter, S. M. Farquhar and K. M. Mullen, *New J. Chem.*, 2004, **28**, 1443.

3 J. S. Lock, B. L. May, P. Clements, J. Tsanaktsidis, C. J. Easton and S. F. Lincoln, *J. Chem. Soc., Perkin Trans. 1*, 2001, 3361; P. R. Ashton, R. Ballardini, V. Balzani, S. E. Boyde, A. Credi, M. T. Gandolfini, M. Gomez-Lopez, S. Iqbal, D. Philp, J. A. Preece, L. Prodi, H. G. Ricketts, J. F. Stoddart, M. S. Tolley, M. Venturi, A. J. P. White and D. J. Williams, *Chem. Eur. J.*, 1997, **3**, 152; V. Balzani, P. Ceroni, A. Credi, M. Gomez-Lopez, C. Hamers, J. F. Stoddart and R. Wolf, *New J. Chem.*, 2001, **25**, 25; R. Corradini, A. Dossena, R. Marchelli, A. Panagia, G. Sartor, M. Saviano, A. Lombardi and V. Pavone, *Chem. Eur. J.*, 1996, **2**, 373; M. B. Nielsen, J. G. Hansen and J. Becher, *Eur. J. Org. Chem.*, 1999, 2807; M. C. Jimenez, C. Dietrich-Buchecker and J.-P. Sauvage, *Angew. Chem., Int. Ed.*, 2000, **39**, 3284; J.-P. Collin, C. Dietrich-Buchecker, P. Gavina, M. C. Jimenez-Molero and J.-P. Sauvage, *Acc. Chem. Res.*, 2001, **34**, 477; B. X. Colasson, C. Dietrich-Buchecker, M. C. Jimenez-Molero and J.-P. Sauvage, *J. Phys. Org.*

Chem., 2002, **15**, 476; T. Hoshino, M. Miyauchi, Y. Kawaguchi, H. Yamaguchi and A. Harada, *J. Am. Chem. Soc.*, 2000, **122**, 9876; S.-H. Chiu, S. J. Rowan, S. J. Cantrill, J. F. Stoddart, A. J. P. White and D. J. Williams, *Chem. Commun.*, 2002, 2948; D. G. Amirsakis, A. M. Elizarov, M. A. Garcia-Garibay, P. T. Glink, J. F. Stoddart, A. J. P. White and D. J. Williams, *Angew. Chem., Int. Ed.*, 2003, **42**, 1126; A. Mirzoian and A. E. Kaifer, *Chem. Commun.*, 1999, 1603; O. P. Kryatova, S. V. Kryatov, R. J. Staples and E. V. Rybak-Akimova, *Chem. Commun.*, 2002, 3014; P. R. Ashton, I. Baxter, S. J. Cantrill, M. C. T. Fyfe, P. T. Glink, J. F. Stoddart, A. J. P. White and D. J. Williams, *Angew. Chem., Int. Ed.*, 1998, **37**, 1294; P. R. Ashton, I. W. Parsons, F. M. Raymo, J. F. Stoddart, A. J. P. White, D. J. Williams and R. Wolf, *Angew. Chem., Int. Ed.*, 1998, **37**, 1913; T. Fujimoto, Y. Sakata and T. Kaneda, *Chem. Commun.*, 2000, 2143.

4 S. J. Rowan and J. F. Stoddart, *Polym. Adv. Technology*, 2002, **13**, 777.

5 H. W. Gibson, L. Hamilton and N. Yamaguchi, *Polym. Adv. Technol.*, 2000, **11**, 791; N. Yamaguchi and H. W. Gibson, *Angew. Chem., Int. Ed.*, 1999, **38**, 143; N. Yamaguchi and H. W. Gibson, *Chem. Commun.*, 1999, 789; N. Yamaguchi and H. W. Gibson, *Macromol. Chem. Phys.*, 2000, **201**, 815; C. Gong and H. W. Gibson, *Macromolecules*, 1996, **29**, 7029; C. Gong and H. W. Gibson, *Macromol. Chem. Phys.*, 1998, **199**, 1801; C. Gong and H. W. Gibson, *Angew. Chem., Int. Ed.*, 1998, **37**, 310; C. Gong, Q. Ji, C. Subramaniam and H. W. Gibson, *Macromolecules*, 1998, **31**, 1814; C. Gong, P. B. Balanda and H. W. Gibson, *Macromolecules*, 1998, **31**, 5278; N. Yamaguchi, L. M. Hamilton and H. W. Gibson, *Angew. Chem., Int. Ed.*, 1998, **37**, 3275; S. Liu, S.-H. Lee, Y. X. Shen and H. W. Gibson, *J. Org. Chem.*, 1995, **60**, 3155; H. W. Gibson, D. S. Nagvekar, J. Powell, C. Gong and W. S. Bryant, *Tetrahedron*, 1997, **53**, 15197; P. E. Mason, W. S. Bryant and H. W. Gibson, *Macromolecules*, 1999, **32**, 1559; T. Azzam, N. A. Peppas, S. Slomkowski and A. J. Domb, *Polym. Adv. Technol.*, 2002, **13**, 788.

6 T. Takata, N. Kihara and Y. Furusho, *Adv. Polym. Sci.*, 2004, **171**, 1.

7 M. J. Gunter, N. Bampos, K. D. Johnstone and J. K. M. Sanders, *New J. Chem.*, 2001, **25**, 166.

8 M. J. Gunter, *Eur. J. Org. Chem.*, 2004, **8**, 1655; K. D. Johnstone, N. Bampos, J. K. M. Sanders and M. J. Gunter, *Chem. Commun.*, 2003, **12**, 1396.

9 Q. Zhang, D. G. Hamilton, N. Feeder, S. J. Teat, J. M. Goodman and J. K. M. Sanders, *New J. Chem.*, 1999, **23**, 897.

10 C. A. Hunter, M. N. Meah and J. K. M. Sanders, *J. Chem. Soc., Chem. Commun.*, 1988, 694; H. L. Anderson, C. A. Hunter and J. K. M. Sanders, *J. Chem. Soc., Chem. Commun.*, 1989, 226; S. Naylor, J. A. Cowan, J. H. Lamb, C. A. Hunter and J. K. M. Sanders, *J. Chem. Soc., Perkin Trans. 2*, 1992, 411; R. J. Harrison, B. Pearce, G. S. Beddard, J. A. Cowan and J. K. M. Sanders, *Chem. Phys.*, 1987, **116**, 429; C. A. Hunter, M. N. Meah and J. K. M. Sanders, *J. Chem. Soc., Chem. Commun.*, 1988, 692.

11 M. R. Johnston and M. J. Latter, *J. Porphyrin Phthalocyanines*, 2002, **6**, 757; R. Kerssebaum, *DOSY and Diffusion by NMR, Bruker Users Guide for XWinNMR 3.1*, 2002; A. Jerschow and N. Muller, *J. Magn. Reson.*, 1996, **123**, 222; A. Jerschow and N. Muller, *Macromolecules*, 1998, **31**, 6573; G. S. Kapur, E. J. Cabrita and S. Berger, *Tetrahedron Lett.*, 2000, **41**, 7181; M. D. Pelta, H. Barjat, G. A. Morris, A. L. Davis and S. J. Hammond, *Magn. Reson. Chem.*, 1998, **36**, 706; K. F. Morris and C. S. Johnson, Jr., *J. Am. Chem. Soc.*, 1992, **114**, 3139; K. F. Morris and C. S. Johnson, Jr., *J. Am. Chem. Soc.*, 1993, **115**, 4291; P. Hodge, P. Monvisade, G. A. Morris and I. Preece, *Chem. Commun.*, 2001, 239; P. J. Skinner, S. Blair, R. Kataky and D. Parker, *New J. Chem.*, 2000, **24**, 265; H. Barjat, G. A. Morris, S. Smart, A. G. Swanson and S. C. R. Williams, *J. Magn. Reson.*, 1995, **108**, 170; D. Wu, A. Chen and C. S. Johnson, Jr., *J. Magn. Reson.*, 1996, **121**, 88; A. Hori, K. Kumazawa, T. Kusukawa, D. K. Chand, M. Fujita, S. Sakamoto and K. Yamaguchi, *Chem. Eur. J.*, 2001, **7**, 4142.

12 K. Yamaguchi, *J. Mass Spectrom.*, 2003, **38**, 473; K. Yamaguchi, S. Sakamoto, *Development of Cold-Spray Ionization Mass Spectrometry and Its Application to Labile Organometallic Compounds in Solution*, http://www.jeol.co.jp/english/technical/coldspray/index.html; S. J. Park, D. M. Shin, S. Sakamoto, K. Yamaguchi, Y. K. Chung, M. S. Lah and J. I. Hong, *Chem. Eur. J.*, 2004, **11**, 235; H. Seki, Y. Sei, K. Shikii, S. Shimotakahara, H. Utsumi, K. Yamaguchi and M. Tashiro, *Anal. Sci.*, 2004, **20**, 1467.

13 A. Hori, K. Kumazawa, T. Kusukawa, D. K. Chand, M. Fujita, S. Sakamoto and K. Yamaguchi, *Chem. Eur. J.*, 2001, **7**, 4142.

14 S. J. Cantrill, G. J. Youn and J. F. Stoddart, *J. Org. Chem.*, 2001, **66**, 6857.

15 P. R. Ashton, I. W. Parsons, F. M. Raymo, J. F. Stoddart, A. J. P. White, D. J. Williams and R. Wolf, *Angew. Chem., Int. Ed.*, 1998, **37**, 1913; M. C. Jimenez, C. Dietrich-Buchecker and J.-P. Sauvage, *Angew. Chem., Int. Ed.*, 2000, **39**, 3284; J.-P. Collin, C. Dietrich-Buchecker, P. Gavina, M. C. Jimenez-Molero and J.-P. Sauvage, *Acc. Chem. Res.*, 2001, **34**, 477; B. X. Colasson, C. Dietrich-Buchecker, M. C. Jimenez-Molero and J.-P. Sauvage, *J. Phys. Org. Chem.*, 2003, **15**, 476.

16 S. Menzer, A. J. P. White, D. J. Williams, M. Belohradsky, C. Hamers, F. M. Raymo, A. N. Shipway and J. F. Stoddart, *Macromolecules*, 1998, **31**, 295.

17 J. G. Hansen, N. Feeder, D. G. Hamilton, M. J. Gunter, J. Becher and J. K. M. Sanders, *Org. Lett.*, 2000, **2**, 449.